EFFECT OF SURFACTANT AND SODIUM ALGINATE MODIFICATION OF GRAPHENE ON THE MECHANICAL AND THERMAL PROPERTIES OF POLYVINYL ALCOHOL (PVA) NANOCOMPOSITES

N. THAYUMANAVAN,[*] PANKAJ TAMBE[*,**,***] and GIRISH JOSHI[**,****]

[*]*School of Mechanical and Building Sciences, VIT University, Vellore – 632014, India*
[**]*Centre for Excellence in Nanocomposites, VIT University, Vellore – 632014, India*
[***]*Centre for Biomaterials Science and Technology, VIT University, Vellore – 632014, India*
[****]*School of Advanced Sciences, VIT University, Vellore – 632014, India*
✉*Corresponding author:PankajTambe,pbtambe2010@gmail.com*

Graphene is under intense investigation as a high performance reinforcing nanofiller for the fabrication of polymer nanocomposites. The challenge is to achieve uniform dispersion of graphene nanosheets and tailor the polymer-graphene nanosheets interface. In this regard, the graphene nanosheetshave been modified using two different non-covalent modifiers, which are sodium dodecyl sulfate (SDS) and sodium alginate (SA). The effect ofthese non-covalent modificationsof graphenenanosheets on the mechanical, thermal and crystallization behavior of polyvinyl alcohol (PVA) nanocompositeshave been studied. The results indicate that the graphenenanosheets areexfoliatedin the PVA matrix, when the graphenenanosheets are modified using SDS and SA. SDS assisted dispersion of graphene nanosheetsdepicts the intercalated state of dispersion of graphenenanosheets in the PVA matrix. This has resulted in remarkable improvement in tensile modulus and tensile strength of PVA nanocomposites containing SDS and SA modified graphenenanosheets, as compared with pure PVA and PVA/SDS-m-graphene nanocomposites. The remarkable increase in mechanical properties is due to an efficient load transfer from PVA to graphenenanosheets, as well as hydrogen bonding between PVA and SA. However,a remarkable increase in the mechanical properties of PVA nanocompositesis achieved despite the decrease in the crystallinity of PVA, revealing the reinforcing efficiency of graphenenanosheets. In addition, the thermal stability of PVA nanocomposites also increases with theaddition of a small concentration of SDS and SA modified graphene.

Keywords: graphene, polyvinyl alcohol (PVA), sodium dodecyl sulfate (SDS), nanocomposites

INTRODUCTION

Graphene is a nanometer thick single atomic layer of graphite, which consists of sp^2-hybridized carbon atoms arranged in a honeycomb lattice with delocalized π electrons.[1]It shows the strongest mechanical strength ever measured, giant intrinsic carrier mobility, record electrical conductivity and thermal conductivity. These remarkable properties of graphene have attracted great interest and possibly become the fastest emerging topic for research.[2-4]Research in the area of graphene-based polymer nanocomposites has been fast boosted owing to the remarkable improvement in the mechanical properties and thermal properties of the nanocomposites by the addition of a low concentration of graphene.[5-11] However, the dispersion quality of graphene and the interfacial interaction between polymer matrix and grapheme need to be addressed to obtain advanced functional nanocomposites. In this regard, covalent and non-covalent modification of graphene has been developed as an effective strategy.[6-8]Covalent modification of graphene has been utilized for improving the dispersion of graphene and maximizing the interfacial interaction between graphene and the polymer matrix. However,the covalent modification strategy creates additional defects within the basal plane of graphene, which damages the structure of the graphitic lattice, deteriorating the inherent properties of grapheme,[12,13]while the non-covalent modification of graphene depicts similar enhancement in the mechanical properties of nanocomposites without creating defects on the structure of the graphitic lattice.[6-7]

Surfactant assisted dispersion of nanoparticles in aqueous solution is one of the most popular

non-covalent modification strategies for a superior dispersion of nanoparticles. Surfactants consist of a hydrophilic head and a long hydrophobic tail. Due to their structure, surfactants tend to migrate to the interface and they also tend to organize themselves into extended structures. The concentration above which micelles are formed is known as critical micelle concentration (CMC); micelles are known to have the ability of solubilizing substances that would otherwise be insoluble or only slightly soluble in a given solvent. By using charged surfactants, such as sodium dodecylsulfate (SDS), the dispersion of carbon nanotubes is stabilized by electrostatic repulsion between the micelles.[14]In the case of charge-neutral surfactants, the dispersion is mainly due to the large solvation shell created by the hydrophilic moieties assembled around the carbon nanotubes.[15] In addition, aqueous solutions of surfactants are more attractive than different toxic solvents like *N*-methyl-pyrrolidone, dimethyl formamide etc. used for the preparation of graphene dispersions,[16] hence the former received greater attention in recent years. Several attempts to exfoliate and disperse graphene in various surfactants have been reported recently.[17,18]

In this paper, dual modifiers have beenused to achieve a finer dispersion of graphene. The dual modifiers used are sodium dodecylsulfate (SDS) and sodium alginate (SA). In addition, polyvinyl alcohol (PVA) is used as a matrix material. It is well known that PVA is used as biomaterial to make hydrogels, high strength films and fibers. So, for modifying graphene, the modifier to be selected must be biocompatible in nature. The chosen dual modifiers, SDS and SA, are biocompatible in nature, as reported earlier in the literature.[19-20] SA is used as a non-covalent modifier due to its biocompatibility, cost-effectiveness, and abundant availability,[19] and SDS for its biocompatibility.[20] This work has been carried out in two stages, to study first the effect of SDS modification ofgraphene on the mechanical properties of PVA nanocomposites,and second the influence of SA and SDS modification of graphene on the mechanical properties of PVA nanocomposites. By thesurfactant assisted strategy,nanocomposites are prepared in two steps to achieve a finer dispersion of graphene in polyvinyl alcohol (PVA), which are (a) ultrasonic pretreatment of graphene in presence of surfactant in aqueous solution, and (b) mixing ultrasonic pretreated graphene suspension into PVA solution. Ultrasonication is required to exfoliate the graphene in the SDS-water solution, which is a common measure to break up aggregates for achieving a finer dispersion of graphene in the surfactant solution. In this work, a high power tip ultasonicatorwas utilized to achieve the finer dispersion of graphene at the optimized surfactant concentration and the dispersability of the graphene was monitored using UV-Vis-NIR spectroscopy. After optimization of sonication parameters and of the surfactant concentration for finer dispersion of graphene, a number of graphene suspensions of different concentrations were prepared under the optimized sonication conditions and subsequently utilized to prepare the PVA nanocomposites. SA was used to stabilize the SDS assisted dispersion of graphene and the stabilized suspensions were mixed with an aqueous solution of PVA to prepare its nanocomposites. An attempt has been made to understand the effect of SDS and SDS+SA modification of graphene on the mechanical properties, thermal stability and crystallization behavior of PVA nanocomposites. Simultaneously, the graphene and nanocomposites were characterized through Fourier transform infrared (FTIR) spectroscopy, X-ray diffraction (XRD), and observedmorphologicallyby scanning electron microscopy (SEM) analysis, transmission electron microscopy (TEM) analysis and optical microscopy analysis.

EXPERIMENTAL
Materials
Graphene (95% purity, mean particle size – 80 nm, average length – 80 nm, average width – 60 nm) was kindly supplied by Quantum Materials Corporation, Banglore. PVA (99% hydrolyzed, Mw ~ 89,000-98,000), sodium alginate powder and sodium dodecyl sulfate (SDS) were purchased from Aldrich.

SDS assisted dispersion of graphene
To achieve the maximum dispersability of graphene in an aqueous solution of SDS surfactant, the graphene suspensions were prepared by adding the as-received graphene material (10 mg) into deionized water (20 mL),in which different amounts of surfactant had been dissolved. The suspensions were ultrasonically treated by using a sonicator(Sonics Vibra Cell, VCX-130, 43% of the maximum output power of 130 Watts and frequency of 20 KHz) for 30 min. Following the centrifugation at 3500 rpm for 15 min at 10,000 g, the upper 80% solutions in the

containers were collected to obtain well-dispersed graphene suspensions free of large aggregates and their absorption was measured. This value was used to quantitatively estimate the graphene concentration in the suspension. In order to evaluate the graphene concentration by absorbance, we measured the absorption coefficient of the graphene/SDS suspensions. For this purpose, we prepared the suspension containing graphene with the concentration of 0.1 mg/mL by adding 10 mg of the as-received graphene material into 100 mL of water containing an optimum amount of surfactant, without centrifugation. This suspension was then diluted into seven different concentrations between 0.005-0.03 mg/mL by adding water. By using a 1-cm path length cuvette, the absorbance was measured while increasing the graphene concentration. The absorption coefficient of the graphene/SDS suspensions was calculated from the Beer–Lambert law.[21]

Synthesis of PVA/SDS-m-graphene nanocomposites

To fabricate PVA/graphene nanocomposites, a desired amount of graphene in an aqueous solution of SDS surfactant was sonicated for 15 minutes and gradually added into 10 wt% PVA aqueous solution and stirred for 8 h, followed by tip sonication for 15 min and bath sonication for 8 hours. After that, the homogeneous PVA/graphene solution was casted into a polystyrene Petri dish, and then dried at 25 °C until the weight was constant. The weight contents of graphene in the composite films were controlled to be 0, 0.1, 0.5 and 1 wt%.

Synthesis of PVA/SDS/SA-m-graphene nano-composites

To fabricate PVA/SA/graphene nanocomposites, a desired amount of graphene in an aqueous solution of SDS surfactant was tip sonicated at an optimized sonication time and gradually added into 10 wt% SA aqueous solution. The ratio of weight percent of graphene to SA was maintained 1:10. The SA/SDS-m-graphene solution was bath sonicated for 4 hours followed by tip sonication for 15 min. Further, the SA/graphene solution was mixed with 10 wt% aqueous solution of PVA and was stirred for 8 h, followed by tip sonication for 15 min and bath sonication for 8 hours. After that, the homogeneous PVA/SA/graphene solution was casted into a polystyrene Petri dish, and then dried at 40 °C until the weight was constant. The weight contents of graphene in the composite films were controlled to be 0, 0.1, 0.5 and 1 wt%.

Characterization

X-ray diffraction (XRD) studies were carried out on a BRUKER, Germany (D8 Advance). The incident X-rays (λ =1.54 nm) from the Cu-target were monochromatized using a Ni filter. XRD patterns were recorded with a step scan with step size of 0.02° between 5° and 40° (2θ). The morphology of the graphene was examined by a JEOL JEM 2100 high resolution transmission electron microscope (HRTEM). The mechanical properties of the films were tested on a Universal Testing Machine, ZwickRoell, Germany, with guage length of 30 mm, width of 10 mm and thickness of 0.1 mm and at a rate of 10 mm/min for 5 films. FTIR spectroscopic analysis of the film samples was carried out with an IRAffinity-1 SHIMADZU (resolution 0.5 cm^{-1}) in the scanning range of 400 to 4000 cm^{-1}. UV-Vis-NIR spectroscopy analysis was carried out by aHITACHI U-2800 spectrophotometer. Scanning electron microscopy (SEM) analysis was performed by a Hitachi S3400, operated at 15 KV with gold sputtering on the tensile fractured samples. Thermogravimetric analysis (TGA) was performed on a Q500 from TA Instruments, with a heating rate of 10°C/min in the temperature range of 25 to 900 °C with nitrogen and air flow of 50 mL/min. The amount of the sample used was 6-8 mg. Based on the original weight loss dependence of the temperature, the first derivative data, i.e. DTG data, were accordingly obtained.

Differential scanning calorimetric (DSC) measurements were carried out using a DSC Q200 from TA Instruments. The cast samples of about 5 mg were dried in a vacuum oven prior to experiment. Temperature and transition heat were calibrated with indium standard. In the 1st heating run, all samples were scanned in the temperature range from 25 °C to 235 °C at a scan rate of 10 K/min under nitrogen atmosphere. Subsequent cooling was recorded in the temperature range from 235 °C to 25 °C at a scan rate of 30 K/min under nitrogen atmosphere. The degree of crystallinity of the PVA phase was calculated from the heat of fusion of the first heating run. The heat of fusion (ΔH_m) of the PVA phase was normalized to the fraction of PVA present in the nanocomposites. The degree of crystallinity (X_c) of the PVA phase was determined from the ratio of normalized heat of fusion ($\Delta H_{m,norm}$) to the heat of fusion of 100% crystalline PVA, (ΔH_m)$_0$, which was taken as 138.6 J/g.[22]

RESULTS AND DISCUSSION
Surfactant assisted dispersion of graphene and its stabilization through sodium alginate

SDS is an anionic surfactant and the ability of SDS to disperse graphene in an aqueous solution was characterized by UV-Vis-NIR absorption spectroscopy. 10 mg of graphene was added into 20 mL of water containing 0.1-2.5 wt% of SDS, followed by sonication, centrifugation, and decantation (80% solution). Figure 1a shows absorbance of the graphene suspensions at a wavelength of 450 nm as a function of SDS concentrations. This wavelength was chosen to avoid the contribution of the SDS molecules to absorption. In Figure 1, the absorbance increases

with an increase in SDS concentration and reaches a maximum, then decreases with higher SDS concentrations. The higher absorbance implies that a larger amount of graphene is suspended in the aqueous solution of SDS. Thus, the SDS concentration at which highest absorbance is observed is chosen as the optimum SDS concentration and the value is 0.55 wt%. The optimum concentration chosen is far greater than the critical micelle concentration of the SDS (7-10 mM) and denoted by a hatched rectangle in Figure 1a. The higher dispersability at a surfactant concentration higher than CMC is due to the fact that the fatty tail of SDS molecules is adsorbed onto the surface of graphene forming a dense coating on hydrophobic graphene nanosheets, as well as micelles. Upon loading the excessive surfactants over their optimum concentrations, the absorbance drops probably due to the flocculation of graphene with excessive surfactants. A similar observation wasmade previously regarding the dispersion of nanoparticles using surfactants.[23-24]

In order to quantitatively evaluate the amounts of graphene dispersed in the aqueous suspensions with the help of SDS, the absorption coefficients of graphene should be calculated first. The initial graphene suspensions were prepared by adding 10 mg of the as-received graphene product into 100 mL of aqueous solution containing the optimum concentrations of SDS (0.55 wt%), as determined from Figure 1a. The graphene suspensions with the initial concentration of 0.1 mg/mL were serially diluted into seven low graphene concentrations in the range of 0.005-0.03 by adding double distilled water. Centrifugation was not performed on these suspensions, because we intended to find out the exact concentrations of graphene in the suspensions. The absorbance of these diluted suspensions with different graphene concentrations was measured at a wavelength of 450 nm using UV-Vis-NIR spectroscopy and is shown in Figure 1b.

The absorbance shows an exactly linear dependency on the graphene concentrations and the slopes of the straight lines are obtained by linear least square regression. The absorption coefficient of the surfactant-stabilized graphene suspensionswas calculated from the slope by using the Beer–Lambert law at a wavelength of 450 nm and was found to be 4356 mL mg^{-1} m^{-1}.

The calculated absorption coefficient was used to estimate the graphene concentrations dispersed in SDS stabilized suspensions. The graphene concentration (C_f) in the suspension stabilized with the optimum amount of surfactant was estimated by using the Beer-Lambert law, $C_f = A/\varepsilon l$, where A, ε and l are absorbance, absorption coefficient, and optical path length, respectively, at a specific wavelength. The calculated graphene concentration at different SDS concentration is shown in Figure 1a. The dispersability of graphene in an aqueous surfactant solution is 0.0026 mg/mL at the optimum surfactant concentration, which is higher than the reported dispersability of graphene in an aqueous solution.[25]

HRTEM was used to observe the state of graphene exfoliation. As may be noted in Figure 2, the graphene nanosheets have wrinkles and a folded region.

Graphene tends to form aggregates due to strong Van der Waals forces of attraction in between the graphene sheets, which significantly affect the mechanical properties of the composites. Optical microscopy has been employed to assess the dispersion quality. Figure 3 shows the optical micrographs of graphene and nanocomposite solutions at different stages of preparation. The mixture of graphene in an aqueous SDS solution shows a poor degree of dispersion through optical microscopy (Figure 3b).

However, dispersion quality improves with the addition of PVA solutions and by further sonication a homogenous nanocomposite solution is obtained (Figure 3c,d). The homogenous mixtures obtained are stable for months (Figure3a).

It is well known that alginate is a product of copolymerization of 2 monomeric units, D-mannuronic acid and L-guluronic acid and it has a linear structure. Generally, these monomers are distributed in the alginate molecule in the form of M blocks or G blocks or with alternating sequences of the MG blocks. Sodium alginate is also water-soluble and dissociates by detaching the sodium as cation and polymer chains as an anion.[25]

When tip sonicated SDS assisted dispersion of graphene is added in the aqueous solution of SA, graphene and SA chains both being negatively charged repel each other and prevent the agglomeration of graphene. Therefore, the nanocomposite solution stays homogeneous, as shown in Figure 4.
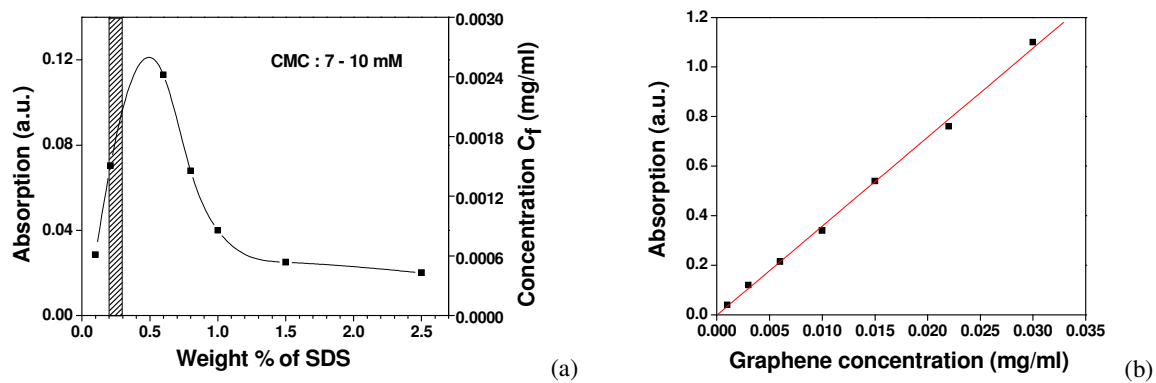
Figure 1: (a) UV-Vis-NIR spectra of aqueous suspensions of graphene stabilized using SDS in different concentration, (b) Absorbance versus graphene concentration in aqueous suspensions stabilized using SDS
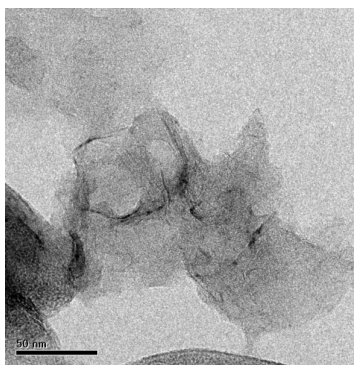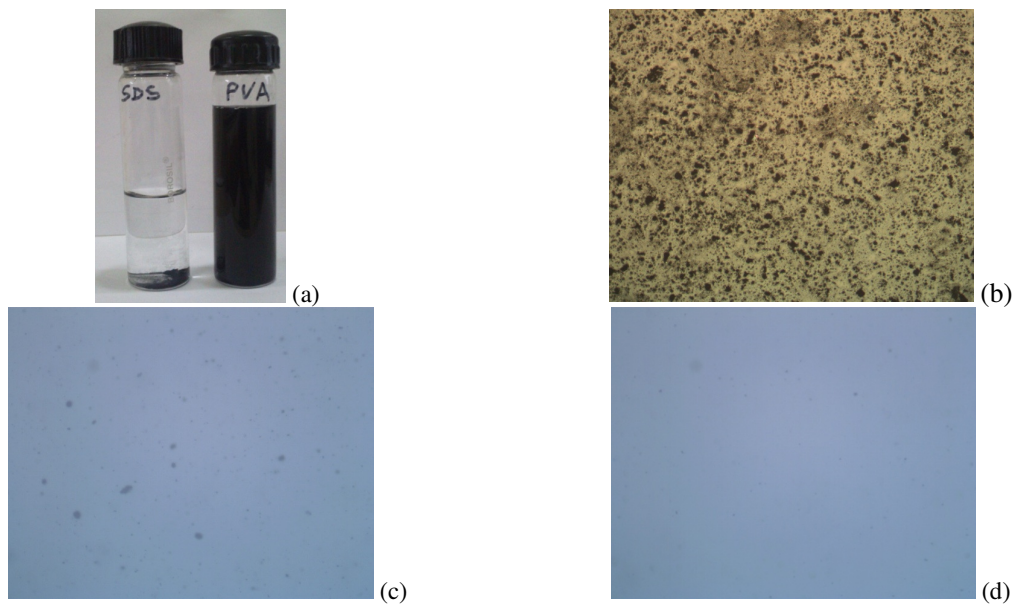

Figure 2: HRTEM images of grapheme

Figure 3: (a) Photograph of graphene and PVA/graphene suspensions and optical micrographs of (b) graphene, (c) PVA/graphene after stirring, (d) PVA/graphene after tip and bath sonication at 200X magnification
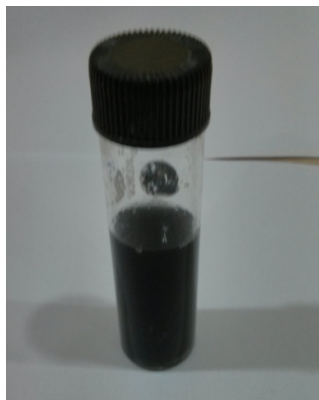
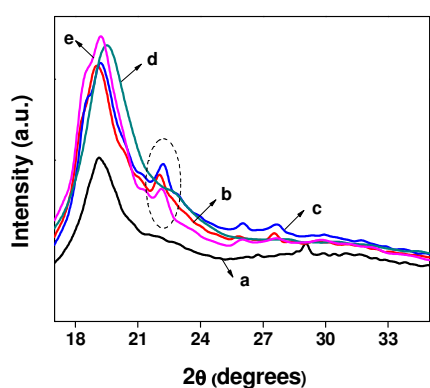Figure 4: Photograph of alginate/graphene suspension

Figure 5: XRD spectra of (a) PVA, (b) PVA+0.5 wt% graphene, (c) PVA+1 wt% graphene, (d) PVA+0.5 wt% SA-m-graphene, (e) PVA+1 wt% SA-m-graphene composites
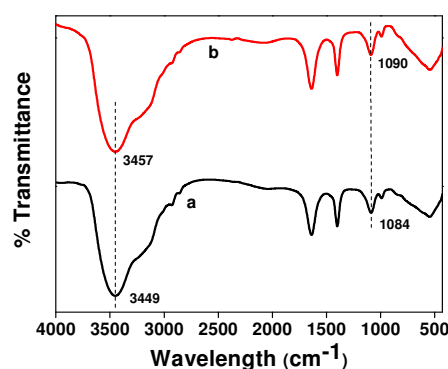

Figure 6: FTIR spectra of (a) PVA and (b) PVA/SA films

XRD and FTIR spectroscopic studies

To probe the state of dispersion of graphene nanosheets in the PVA matrix, XRD was utilized. Figure 5 illustrates the XRD spectra of pure PVA, PVA/SDS/graphene and PVA/SDS/SA-m-graphene nanocomposite films. The typical diffraction of pure PVA appears at $2\theta = 19.1°$, exhibiting (101) crystalline reflection.[26] The XRD pattern of PVA/graphene nanocomposites is similar to that of pure PVA with a peak shift. This peak shift of PVA demonstrates the interaction between PVA and graphene. In addition, PVA/graphene nanocomposites containing 0.5 and 1wt% of SDS assisted dispersed graphene in the PVA matrix show a small peak at ~23°, which exhibits the intercalated nature of the dispersion of graphene nanosheets. The XRD pattern of PVA/SDS/SA-m-graphene nanocomposites is similar to that of pure PVA with a peak shift (Figure 5). This peak shift of PVA demonstrates

the interaction between PVA and SA. PVA/SDS/SA-m-graphene nanocomposites containing 0.5wt% of graphene do not present the small peak at ~23°, which demonstrates the exfoliated nature of the dispersion of graphene nanosheets. Meanwhile, the XRD spectrum of the 1wt% SA modified graphene depicts the peak at ~23°, showing an intercalated nature of the dispersion of graphene nanosheets in the PVA nanocomposites. These results demonstrate that SA helps in a finer dispersion of graphene nanosheets in the PVA matrix and is expected to influence the mechanical properties of PVA nanocomposites significantly.

FTIR experiments were performed to determine the interaction between PVA and SA. It is well known that the band corresponding to –C–OH stretching (around 1084 cm^{-1}) and -OH stretching (between 3100-3500 cm^{-1}) bands are sensitive to the hydrogen bonding.[6]Figure 6

shows the band shifts with the addition of SA in the PVA. These results suggest that there exists hydrogen bonding between PVA and SA. Thus, it is expected that by the addition of surfactant assisted dispersed graphene and sodium alginate modified graphene will influence the mechanical behavior, crystallization behavior and thermal stability of PVA nanocomposites,which isdiscussed subsequently.

DSC and TGA studies

It is well known that the PVA degrades near the melting temperature and degradation lowers the crystallization temperature. In addition, it was observed that at a higher cooling rate, less degradation takes place.[27] This is the reason why DSC studies were carried out at the heating rate of 10 K/min and cooling rate of 30 K/min. Figure7a shows the crystallization exotherms of pure PVA, PVA/SDS-m-graphene and PVA/SDS/SA-m-graphene nanocomposite films. The crystallization temperature (T_c) of PVA increases in the presence of SDS assisted dispersed graphene, as compared to pure PVA (Table 1, Figure 7a). This is due to the adsorption of SDS onto the graphene, depicting a heterogenous nucleating effect of the SDS wrapped graphene. The SA modified and SDS assisted dispersed graphene PVA nanocomposites showed higher T_c, as compared to PVA/SDS-m-graphene nanocomposites and pure PVA. This may be due to the wrapping of SA chains over graphene nanosheets and the formation of the hydrogen bond between PVA and SA, which results in increased T_c, as compared to that of pure PVA and PVA/SDS-m-graphene nanocomposites. Table 1 shows that the rate of crystallization of PVA increased in the presence of SDS assisted dispersed graphene with and without modification with SA, as the parameter $T_{onset} - T_c$ is found to

decrease in PVA nanocomposites. On the basis of these observations, it may be concluded that graphene influences the crystalline morphology in the PVA/SDS-m-graphene nanocomposites with and without modification by SA.

The melting endotherms of pure PVA, PVA/SDS-m-graphene and PVA/SDS/SA-m-graphene nanocomposite films exhibit a single melting endothermic peak (T_m) in the second heating run of DSC scans (Figure7b). The T_m of PVA/SDS-m-graphene nanocomposites with and without modification by SA indicates a decrease. The degree of crystallinity (X_c) calculated from the normalized heat of fusion from the second heating cycle of DSC is listed in Table 1. X_c is found to decrease remarkably in PVA/SDS-m-graphene and PVA/SDS/SA-m-graphene nanocomposites, as compared to pure PVA, demonstrating that graphene dispersion and its interaction with SDS and SA influence the crystallization behavior of PVA.

TGA is used to characterize the thermal properties of pure PVA, PVA/SDS-m-graphene and PVA/SDS/SA-m-graphene nanocomposite films. Figure 8 shows the TG and DTG curves of the PVA, PVA/SDS-m-graphene and PVA/SDS/SA-m-graphene nanocomposites under nitrogen atmosphere at a heating rate of 10ºC/min. All TG curves (Figure 8a) present a thermal decomposition process in two steps, in the temperature range 25-700ºC.

The decomposition region is centered between 200-520ºC and the temperature of the maximum degradation rate for the nanocomposites (obtained from the derivative of TGA curves, Figure 8b) are about ~1.5ºC higher than that of pure PVA in the case of PVA/SDS-m-graphene nanocomposites, and ~2.5ºC higher than that of pure PVA in the case of PVA/SDS/SA-m-graphene nano-composites.

Table 1
Melting and crystallization parameters of PVA, PVA/graphene and PVA/SA-m-graphene nanocomposite films

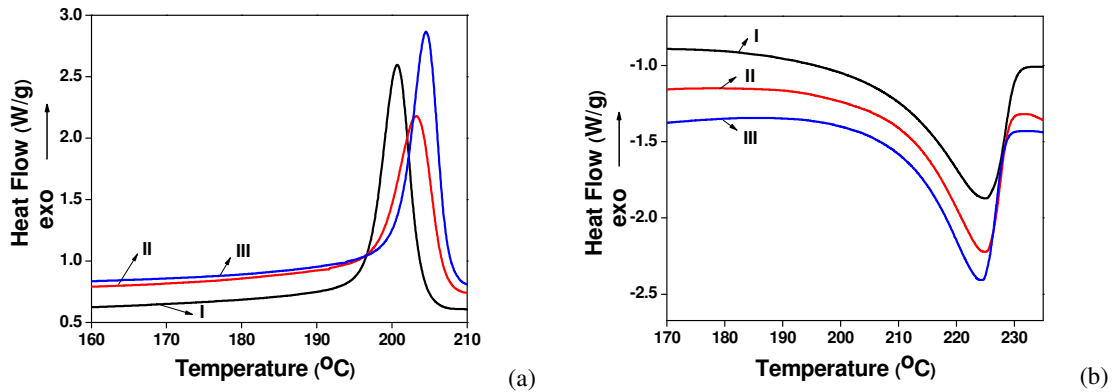| Sample codes	T_m (°C)	$(\Delta H_m)_{nor}$ (J/g)	X_c (%)	T_{onset}(°C)	T_c (°C)	$T_{onset}-T_c$ (°C)
PVA	225.2	84.4	60.8	208.4	200.6	7.8
PVA+0.1 wt% graphene	224.8	69.5	52.3	209.4	203.8	7.5
PVA+0.5 wt% graphene	224.6	68.1	51.4	209.9	203.3	6.6
PVA+1 wt% graphene	224.4	57.7	43.8	205.5	197.2	5.9
PVA+SA+0.1 wt% graphene	224.3	69.9	52.5	209.9	204.6	5.3
PVA+ SA+0.5 wt% graphene	224.9	75.5	56.7	211.8	205.7	6.1
PVA+ SA+1 wt% graphene	225.1	68.7	51.6	214.1	207.4	6.7

Figure 7: DSC (a) crystallization exotherms and (b) melting endotherms of (I) PVA phase in pure PVA, (II) PVA/0.1 wt% graphene nanocomposites, (III) PVA/0.1 wt% SA-m-graphene nanocomposites
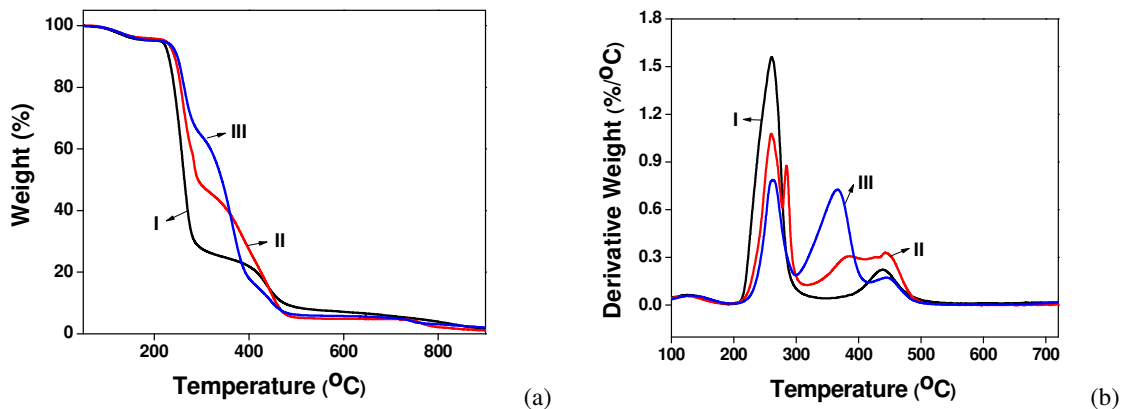

Figure 8: (a) TGA and (b) DTG curves of (I) PVA phase in pure PVA, (II) PVA/0.1 wt% graphene nanocomposites, (III) PVA/0.1 wt% SA-m-graphene nanocomposites

An improvement in the thermal stability of PVA is achieved even at low concentration dispersion of SDS-m-graphene and PVA/SDS/SA-m-graphene nanocomposites.

Mechanical properties and morphological observation

It is expected that the addition of graphene, which has an exceptionally high Young's modulus,into the PVA matrix will have a significant reinforcing effect on the mechanical properties of the nanocomposites. Table 2 shows the results of tensile tests. It is clearly seen that the Young's modulus of the PVA nanocomposite with 0.5wt% SDS assisted dispersed graphene is the highest, which can be attributed to the efficient load transfer from the graphene to the PVA matrix. The tensile modulus of the pure PVA was 0.39±0.005 GPa and it increased to 0.58±0.006 GPa (0.1 wt% graphene content, increased by 48.3%), 0.99±0.005 GPa (0.5 wt% graphene content, increased by 151.8%) and to 0.84±0.004 GPa (1 wt% graphene content,

increased by 113.6%). In addition, the tensile strength of the pure PVA was 40±3 MPa and it increased to 64±3 MPa (0.1 wt% graphene content, increased by 55.8%), 70±2 MPa (0.5 wt% graphene content, increased by 67.4%) and to 59±3 MPa (1 wt% graphene content, increased by 44.2%). In summary, the tensile strength and tensile modulus of the nanocomposites increased with the increase of the graphene loadings up to 0.5 wt% SDS assisted dispersed graphene. This may be due to the efficient load transfer from PVA to the graphene nanosheets. The elongation at break of the composites gradually increases with graphene loading. The reason may be attributed to the fact that the intercalated nature of SDS assisted dispersed graphene in the PVA matrix undergoes slippage under tensile loading. It is to be noted that the elongation at break did not decrease remarkably even after adding 1 wt% of graphene, exhibiting ductile behavior, which is due to the decrease in crystallinity of PVA. The improvement in mechanical properties despite the decrease in crystallinity shows the reinforcing

efficiency of SDS assisted dispersion of graphene on the mechanical properties of PVA nanocomposites.

With the addition of SDS/SA modified graphene in the 1:10ratio of graphene to SA, a remarkable improvement in Young's modulus and tensile strength of the PVA nanocomposites is recorded as compared to pure PVA. Young's modulus is the highest for the PVA/SDS/SA-m-graphene nanocomposite with 0.5 wt% of SDS and SA modified graphene loading. It is to be noted that SDS and SA modified graphene/PVA nanocomposites show a remarkable improvement in mechanical properties, as compared to the PVA/SDS modified graphene nanocomposites. The remarkable improvement in Young's modulus and tensile strength of the PVA nanocomposites using SDS and SA modified graphene is due to the exfoliated nature of graphene dispersion and hydrogen bonding in between SA and PVA, which has resulted in efficient load transfer from graphene to the PVA matrix. However, higher concentration of SDS and SA modified graphene (1 wt%) leads to decreased mechanical properties, which is due to the increasing SA content in the PVA matrix. This may be due to the intercalated graphene dispersion at higher concentration in PVA/SA-m-graphene nanocomposites. The remarkable increase in mechanical properties is due to the graphene, as evident from the slight increase in mechanical properties in the case of the PVA/SA film containing 10 wt% of SA and the PVA/SDS film. The tensile modulus of the pure PVA was 0.39±0.005 GPa and it increased to 0.89±0.005 GPa (0.1 wt% graphene content, increased by 126.5%), 1.91±0.006 GPa (0.5 wt% graphene content, increased by 385.1%) and to 1.86±0.005 GPa (1 wt% graphene content, increased by 372.1%). In addition, the tensile strength of the pure PVA was 40±3 MPa and it increased to 69±3 MPa (0.1 wt% graphene content, increased by 67.4%), 88±3 MPa (0.5 wt% graphene content, increased by 111.6%) and to 83±2 MPa (1 wt% graphene content, increased by 97.7%).

To study the distribution of graphene nanosheets in the PVA matrix, the Halpin-Tsai equation is widely used to simulate the modulus for anisotropic nanofiller reinforced polymer composites.[38,29]

Thus, the modified Halpin-Tsai equation can be used to estimate the orientation of the graphene sheets in the PVA nanocomposites as follows:

$$E_r = E_p \left[\frac{3}{8} \frac{1 + (2l_G/t_G)\eta_L V_G}{1 - \eta_L V_G} + \frac{5}{8} \frac{1 + 2\eta_T V_G}{1 - \eta_T V_G} \right]$$

$$E_{//} = E_p \left[\frac{1 + (2l_G/t_G)\eta_L V_G}{1 - \eta_L V_G} \right]$$

$$\eta_L = \frac{(E_G/E_p) - 1}{(E_G/E_p) + 2l_G/t_G}$$

$$\eta_T = \frac{(E_G/E_p) - 1}{(E_G/E_p) + 2}$$

Here the E_r and $E_{//}$ are Young's modulus values for the nanocomposites with randomly distributed graphene nanosheets, and aligned parallel to the surface, respectively; E_P and E_G are Young's modulus values for PVA by tensile testing and graphene of about 1 TPa[3], respectively; l_G, t_G and V_G refer to the length, thickness and volume fraction of graphene in the nanocomposites. The length and thickness of graphene can be considered to be 80 nm and 1 nm, respectively.

A Cox's modified model[30] can be used to calculate Young's modulus for the composites with tailored interface, and written as follows:

$$\beta = \frac{2l_G}{t_G} \sqrt{\frac{E_P}{(1+\nu)E_G \times \ln(4/\pi V_f)}}$$

$$E = (1 - V_f)E_P + q\left(1 - \frac{\tanh \beta}{\beta}\right)E_G V_f$$

where β is interfacial shear stress transfer and q is the orientation factor of graphene, ν is the Poission ratio of PVA and is assumed to be 0.33.[31]

Young's modulus for the SDS assisted dispersed graphene in PVA nanocomposites with different graphene orientations are calculated using modified Halpin-Tsai equations and compared with the experimental results, as shown in Figure 9. It seems that the theoretical simulation for the unidirectional distribution of graphene nanosheets is consistent with the experimental data, when the graphene loading is as low as 0.1 wt% in the PVA composites. This can be explained by the fact that the graphene nanosheets are easily aligned parallel to the surface of the PVA composite films because of the following reasons: (a) graphene nanosheets are inclined to lie flat during the solution casting process due to their high aspect ratio and (b) the steric hindrance between graphene sheets themselves would be low at such a low graphene loading level.[32,33] With an increase in graphene loading, the graphene nanosheets are most likely dispersed randomly in the PVA matrix, especially at higher graphene loadings. The values of

Young's modulus for the SDS and SA modified graphene dispersed in PVA nanocomposites with different graphene orientations are calculated using Cox's modified model and compared with the experimental results, as shown in Figure 10.

Table 2
Mechanical properties of PVA, PVA/graphene and PVA/SA-m-graphene nanocomposites films

| Sr. No	Sample codes	Mechanical properties		
		Tensile strength (MPa)	Modulus (GPa)	Elongation at break (%)
1	PVA	40±3	0.39±0.005	85±6
2	PVA+0.1 wt% graphene	64±3	0.58±0.006	96±5
3	PVA+0.5 wt% graphene	70±2	0.99±0.005	120±6
4	PVA+1 wt% graphene	59±3	0.84±0.004	130±4
5	PVA+SA+0.1 wt% graphene	69±3	0.89±0.005	98±5
6	PVA+SA+0.5 wt% graphene	88±3	1.91±0.006	116±6
7	PVA+SA+1 wt% graphene	83±2	1.86±0.005	116±6
8	PVA+10 wt% SA	59±3	0.56±0.003	84±7
9	PVA+SDS	46±2	0.46±0.004	92±4
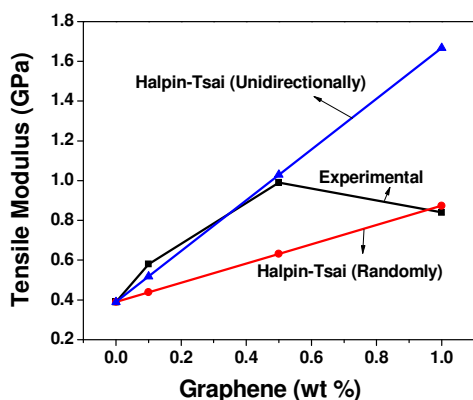
Figure 9: Experimental tensile modulus of nanocomposites; calculated data derived from Halpin-Tsai model under the hypothesis that graphene sheets are randomly distributed in the composites and aligned parallel to the surface of the nanocomposite films
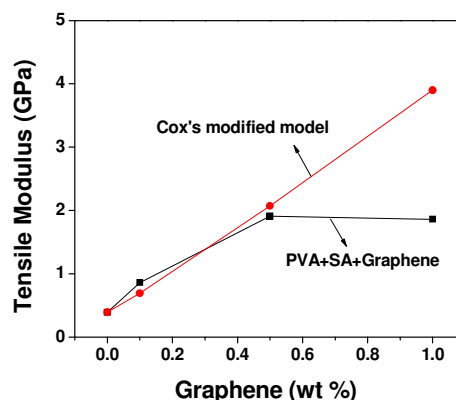

Figure 10: Experimental tensile modulus of nanocomposites; calculated data derived from Cox's modified model under the hypothesis that graphene sheets are aligned parallel to the surface of the nanocomposite films
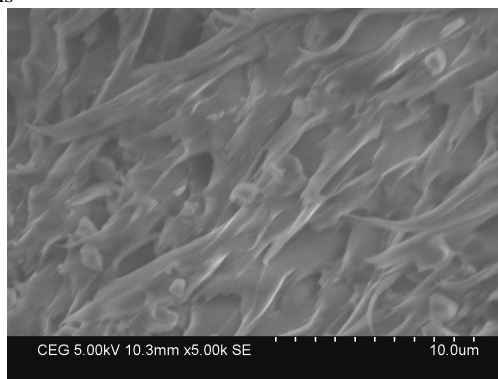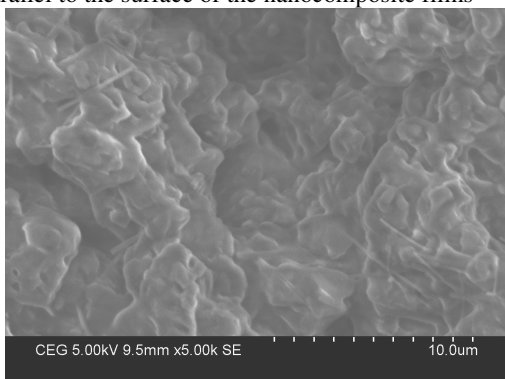

Figure 11: SEM images of fracture surface of (a) PVA/graphene nanocomposite films containing 1 wt% SDS assisted dispersed graphene; (b) PVA/graphene nanocomposite films containing 1 wt% SDS assisted dispersed and SA modifiedgraphene

The theoretical simulation by assuming unidirectional orientation of graphene nanosheets is consistent with the experimental data, when the SDS/SA modified graphene loading is as low as

0.1 wt% in the PVA nanocomposites. At higher SA modified graphene loading, the graphene nanosheets are most likely dispersed randomly in the PVA matrix, especially at higher graphene loadings.

The fracture surfaces of the PVA/SD-m-graphene and PVA/SDS/SA-m-graphene nanocomposite films are further investigated by SEM after tensile testing. As shown in Figure 11, SEM images of the fracture surfaces of the PVA/graphene nanocomposite films clearly reveal the adhesion of graphene to the PVA matrix without any graphene nanosheets pulled out.

CONCLUSION

In conclusion, the intercalated dispersion ofSDS assisted dispersed graphene in PVA nanocomposite films was successfully prepared. The addition of SDS assisted dispersed graphene significantly decreased the crystallinity of nanocomposites, which resulted in ductile nanocomposite film.The enhancement in mechanical properties is due to the intercalated dispersion and effective stress transfer from graphene nanosheets to the PVA matrix. The tensile modulus and strength of the PVA nanocomposites with 0.5 wt% of graphene were by 151.8% and 67.4% higher than those of pure PVA. The addition of graphene also improved the thermal stability of the PVA nanocomposites.

SDS assisted dispersed graphene was successfully stabilized using SA and thereafter added to the PVA solution to prepare PVA nanocomposites. There was hydrogen bonding between PVA and SA. This resulted in a remarkable improvement in the mechanical properties of PVA/SDS/SA-m-graphene nanocomposites, despite thedecrease in crystallinity of PVA, by facilitating a better load transfer from graphene to the PVA matrix. However, the decrease in the crystallinity of PVA was lower in the case of SA and SDS modified graphene as compared to that of SDS modified graphene in the PVA nanocomposites. The tensile modulus and tensile strength of the PVA nanocomposites with 0.5 wt% of SA and SDS modified graphene were the highest (385.1% and 111.6% higher than those of pure PVA) due to well exfoliated graphene nanosheets, established through XRD. The addition of SA and SDS modified graphene also improved the thermal stability of the PVA nanocomposites remarkably, as compared to PVA and SDS modified graphene.

REFERENCES

[1] A. K. Geim and K. S. Novoselov, *Nat. Mater.*, **6**, 183 (2007).
[2] K. S. Novoselov, A. K. Geim,S. V. Morozov,D. Jiang,Y. Zhang*et al.*, *Science*, **306**, 666 (2004).
[3] C. G. Lee, X. D. Wei, J. W. Kysar, J. Hone, *Science*, **321**, 385 (2008).
[4] A. A. Balandin, G. Suchismita, B. Wenzhong,C. Irene,T. Desalegne *et al.*, *Nano Lett.*, **8**, 902 (2008).
[5] X. Yuxi, H. Wenjing, B. Hua, L. Chun, S. Gaoquan, *Carbon*, **47**, 3538 (2009).
[6] T. ZhenghaI, L. Yanda, G. Baochun, Z. Liqun, J. Demin, *Polymer*, **53**, 673 (2012).
[7] G. Juan, R. Lulu, W. Ruiyu, Z. Chao, Y. Yang, L. Tianxi, *Compos.: Part B*, **42**, 2130 (2011).
[8] K. L. Rama, S. Sanjoy, K. N. Arun, *Carbon*, **50**, 815 (2012).
[9] Z. Tiannan, C. Feng, T. Changyu, B. Hongwei, Z. Qin *et al.*, *Compos. Sci. Technol.*, **71**, 1266 (2011).
[10] Y. Xiaoming, L. Liang, S. Songmin, T. Xiao-ming, *Polymer*, **51**, 3431 (2010).
[11] L. Yuanqing, U. Rehan, A. S. Yarjan, Z. Lianxi, L. Kin, *Carbon*, **55**, 321 (2013).
[12] S. Stankovich, D. A. Dikin, G. H. B. Dommett, K. M. Kohlhaas, E. J. Zimney *et al.*, *Nature*, **442**, 282 (2006).
[13] H. Kim, S. Kobayashi, M. A. AbdurRahim, M. J. Zhang, A. Khusainova *et al.*, *Polymer*, **52**, 1837 (2011).
[14] M. J. O'Connell, S. H. Bachilo, C. B. Huffman, V. C. Moore, M. S. Strano *et al.*, *Science*, **297**, 593 (2002).
[15] V. C. Moore, M. S. Strano, E. H. Haroz, R. H. Hauge, R. E. Smalley *et al.*, *NanoLett.*, **3**, 1379 (2003).
[16] M. Hsiao, S. Liao, M. Yen, P. Liu, N. Pu *et al.*, *ACS Appl. Mater. Inter.*, **2**, 3092 (2010).
[17] M. J. Fernandez-Merino, J.I. Paredes, S. Villar-Rodil, L. Guardia,P. Solıs-Fernandez *et al.*, *Carbon*,**50**, 3184 (2012).
[18] R. J Smith, M. Lotya, J. N. Coleman, *New J.Phys.*, **12**,125008 (2010).
[19] Y. Qin, *Polym.Int.*,**57**, 171 (2008).
[20] R. P. Subbiah, H. Lee, M.Veerapandian, S. Sadhasivam, S. W. Seo *et al.*, *Anal. Bioanal. Chem.*, **400**,5 47 (2011).
[21] L. D. S. Yadav, "Organic Spectroscopy", Netherlands, Kluwer Academic Publishers, 2005, pp. 7-8.
[22] J. X. Su, Q. Wang, R. Su, K. Wang, Q. Zhang, Q. Fu, *J. Appl.Polym.Sci.*, **107**, 4070 (2008).

[23]R. Rastogi, R. Kaushal, S. K. Tripathi, A. L. Sharma, I. Kaur, L. M. Bharadwaj, *J. Colloid. Interface Sci.*, **328**, 421 (2008).

[24]J. C.Goak, S. H. Lee, J. H. Han, S. H. Jang, K. B. Kim,Y. Seo *et al.*, *Carbon*, **49**, 4301 (2011).

[25] P. Sriamornsak, S. Sungthongjeen, *Aaps Pharmscitech.*, **8**, 1 (2007).

[26] Z. L. Yao, N. Braidy, G. A. Botton, A. Adronov, *J. Am. Chem. Soc.*,**125**, 16015 (2003).

[27] Z. Wang, PhD Thesis, University of London, 2007.

[28] J. Liang, Y. Huang, L. Zhang, Y. Wang, Y. Ma *et al.*, *Adv. Funct. Mater.*, **19**, 2297 (2009).

[29] X. Zhao, Q. Zhang, D. Chen, P. Lu, *Macromolecules*, **43**, 2357 (2010).

[30] G. G. Tibbetts, J. J. McHugh, *J. Mater. Res.*, **14**, 2871 (1999).

[31] K. Urayama, T. Takigawa, T. Masuda, *Macromolecules*, **26**, 3092 (1993).

[32] C. Zhang, W. T. Weng, F. Wei, H. Shu, T. Liu, *J. Mater. Chem.*, **22**, 11748 (2012).

[33]N. Thayumanavan, P. B.Tambe, G. Joshi, M. Shukla, *Compos. Interface.*, DOI: 10.1080/ 15685543. 2014.879512 (2014).